Wet Chemical Approaches to Patterned Arrays of Well-Aligned ZnO Nanopillars Assisted by Monolayer Colloidal Crystals

Cheng Li,[†] Guosong Hong,[†] Pengwei Wang,[‡] Dapeng Yu,[‡] and Limin Qi*,[†]

Beijing National Laboratory for Molecular Sciences (BNLMS), State Key Laboratory for Structural Chemistry of Unstable and Stable Species, College of Chemistry, and Electron Microscopy Laboratory, State Key Laboratory for Mesoscopic Physics, School of Physics, Peking University, Beijing 100871, People's Republic of China

Received October 18, 2008. Revised Manuscript Received January 5, 2009

Hexagonally patterned arrays of well-aligned, regular ZnO nanopillars with controlled size, shape, and orientation were directly fabricated on zinc foils via a facile wet chemical approach with the assistance of monolayer colloidal crystals (MCC). Two kinds of templates that were derived from MCC, i.e., inverted MCC (IMCC) and connected MCC (CMCC), were employed as masks to define the growth sites and spaces on zinc foils for the realization of site-specific patterned growth of ZnO nanopillars. Individually patterned arrays of ZnO nanopillars (i.e., one ZnO nanopillar growing at one single growth site) were readily produced. Interestingly, the vertically aligned ZnO nanopillars were also side-oriented, indicating a quasi-epitaxial growth on the zinc substrate. The diameter of the ZnO nanopillars can be controlled in a wide range from 60 to 900 nm by varying the structural parameters of the MCC templates and the growth conditions. Moreover, by decreasing the reaction solution concentration, a bundle of ZnO nanorods rather than an individual nanopillar were selectively grown at one single growth site. The as-grown ZnO nanopillar arrays were well-crystallized and exhibited strong excitonic emission and weak defect-related emission at room temperature, which promises their potential applications in optical devices such as stimulated emitters and lasing cavities.

Introduction

Controlled patterning of nanostructured materials on surfaces has become increasingly important because of the ever-decreasing dimensions of various devices, including those used in electronics, optoelectronics, electrochemistry, and electromechanics.[1,2] Nanostructures of ZnO have attracted both scientific and industrial interest owing to the possibility of device assembly and manipulation in the nanometer regime.[3−5] Among the various nanoforms of ZnO, quasi- one-dimensional (1D) structures such as nanowires, nanorods, nanopillars, nanopins, and nanotubes have stimulated intensive interests because of their unique semiconducting and piezoelectric properties.[6] In particular, the alignment of such 1D ZnO nanostructures into ordered nanoarrays can bring about improved performance in various promising areas such as piezo-nanogenerators,[3] UV lasers,[7] dye sensitized solar cells,[8] antireflection coatings,[9] and photocatalysis.[10] However, for the realization of these potential applications, facile low-temperature growth techniques and precise control over size, shape, orientation, and pattern (location and spacing) of the 1D ZnO nanostructures are highly desirable.

Until now, signifcant effort has been made in the patterned growth of 1D ZnO nanostructures by high-temperature vapor phase methods, where patterned growth was realized by controlling the size and location of metal catalysts or oxide seed layer on a substrate surface using various patterning techniques including photolithography,[7,11,12] e-beam lithography,[13] laser-interference lithography,[14] anodic aluminum oxide tempating,[15,16] block copolymer micelles,[17] and nano-

* To whom correspondence should be addressed. E-mail: liminqi@pku.edu.cn. Fax: +86-10-62751708.
[†] College of Chemistry.
[‡] School of Physics.

(1) Henzie, J.; Barton, J. E.; Stender, C. L.; Odom, T. W. *Acc. Chem. Res.* **2006**, *39*, 249.
(2) Fan, H. J.; Werner, P.; Zacharias, M. *Small* **2006**, *2*, 700.
(3) (a) Wang, Z. L.; Song, J. *Science* **2006**, *312*, 242. (b) Wang, X.; Song, J.; Liu, J.; Wang, Z. L. *Science,* **2007**, *316*, 102. (c) Qin, Y.; Wang, X.; Wang, Z. L. *Nature* **2008**, *451*, 809.
(4) Klingshirn, C. *ChemPhysChem* **2007**, *8*, 782.
(5) Schmidt-Mende, L.; MacManus-Driscoll, J. L. *Mater. Today* **2007**, *10*, 40.
(6) (a) Wang, Z. L. *J. Nanosci. Nanotechnol.* **2007**, *8*, 27. (b) Wang, Z. L. *Mater. Today* **2007**, *10*, 20.
(7) (a) Huang, M. H.; Mao, S.; Feick, H.; Yan, H. Q.; Wu, Y. Y.; Kind, H.; Weber, E.; Russo, R.; Yang, P. D. *Science* **2001**, *292*, 1897. (b) Yang, P. D.; Yan, H.; Mao, S.; Russo, R.; Johnson, J.; Saykally, R.; Morris, N.; Pham, J.; He, R.; Choi, H.-J. *Adv. Funct. Mater.* **2002**, *12*, 323.
(8) Law, M.; Greene, L. E.; Johnson, J. C.; Saykally, R.; Yang, P. D. *Nat. Mater.* **2005**, *4*, 455.
(9) Lee, Y.-J.; Ruby, D. S.; Peters, D. W.; McKenzie, B. B.; Hsu, J. W. P. *Nano Lett.* **2008**, *8*, 1501.
(10) Wang, G.; Chen, D.; Zhang, H.; Zhang, J. Z.; Li, J. H. *J. Phys. Chem. C* **2008**, *112*, 8850.
(11) Greyson, E. C.; Babayan, Y.; Odom, T. W. *Adv. Mater.* **2004**, *16*, 1348.
(12) Conley Jr, J. F.; Stecker, L.; Ono, Y. *Nanotechnology* **2005**, *16*, 292.
(13) Ng, H. T.; Han, J.; Yamada, T.; Nguyen, P.; Chen, Y. P.; Meyyappan, M. *Nano Lett.* **2004**, *4*, 1247.
(14) Kim, D. S.; Ji, R.; Fan, H. J.; Bertram, F.; Scholz, R.; Dadgar, A.; Nielsch, K.; Krost, A.; Christen, J.; Gösele, U.; Zacharias, M. *Small* **2007**, *3*, 76.
(15) Chik, H.; Liang, J.; Cloutier, S. G.; Kouklin, N.; Xu, J. M. *Appl. Phys. Lett.* **2004**, *84*, 3376.
(16) Fan, H. J.; Lee, W.; Hauschild, R.; Alexe, M.; Rhun, G. L.; Scholz, R.; Dadgar, A.; Nielsch, K.; Kalt, H.; Krost, A.; Zacharias, M.; Gösele, U. *Small* **2006**, *2*, 561.

10.1021/cm802839u CCC: $40.75
Published on Web 01/30/2009

spheres lithography.[18−21] Though vapor phase growth methods bear lots of advantages, wet chemical approaches are appealing for reasons of large-scale production, cost-efficiency, environmental friendliness, and compatibility with general substrates.[22,23] Many efforts have been devoted to the patterned growth of 1D ZnO nanostructure arrays employing low-temperature aqueous solution methods; in particular, ZnO seed layers prepatterned via e-beam lithography,[23−28] photolithography,[29] and micromolding[30,31] are commonly used for the subsequent ZnO growth. In these procedures, the step of coating ZnO seed layers on nonepitaxial substrates by sol−gel process, thermal evaporation, or atomic layer deposition before patterning is inevitable and thus may increase the complexity of the experimental procedure. Notably, a biomimetic route has also been exploited to control the nucleation and assembly of micropatterned ZnO nanorod arrays using patterned self-assembled monolayers on silver substrates[32] or selectively functionalized flexible plastic substrates.[33] However, most of the studies demonstrated the growth of a set of nanowires rather than an individual nanowire on each growth site. Relying on high-resolution electron beam writing, individually patterned ZnO can be grown,[23] but large-scale patterning would be very expensive and time-consuming. Besides, these strategies involving growth on seeded areas have exerted limited control over the alignment and crystal quality of ZnO nanowire at a single growth site. For the production of uniform devices for applications such as microelectron beams, it is crucial to integrate uniform arrays of individual single crystal nanowires with controllable size and location. By epitaxial hydrothermal growth on partially masked substrates such as GaN, spinel, or sapphire, high-quality ZnO microrod, microtunnels, and microcrystals can be obtained;[34,35] however, there are only few reports on the epitaxial growth of 1D ZnO crystals with submicrometer diameters.[23] Therefore, it remains a great challenge to develop facile solution routes to the individually patterned growth of well-aligned, 1D ZnO nanostructures with good uniformity and high crystal quality.

Nanosphere lithography that usually employs monolayer colloidal crystals (MCC) as the mask has been proven to be a flexible and cost-effective technique for the patterning of nanostructured arrays with long-range periodicity in a large scale.[36] As already mentioned above, it has been successfully used in the arrangement of gold catalyst on substrates in vapor phase growth of ZnO,[18−21] but the MCC templating method has been rarely applied in a catalyst-free solution growth system to control the patterned growth of 1D ZnO nanostructures. On the other hand, the direct growth of oriented ZnO nanorod and nanotube arrays on a zinc substrate was recently realized by oxidation in solution at room temperature or under hydrothermal conditions;[37−40] moreover, large-scale ultrathin nanofibers,[41] ultralong nanowire/belts,[42] and pine-nanotree arrays[43] were directly grown on zinc foils. Though the growth of 1D ZnO nanostructures directly on zinc foils in solution has already been successfully demonstrated, patterned growth on masked Zn foil has not been reported yet.

In this work, we demonstrate the controlled growth of well-aligned, individually patterned, regular ZnO nanopillars assisted by monolayer colloidal crystal (MCC) on zinc foil via a wet chemical method. We chose zinc foils as the substrate for the assembly of MCC and the subsequent ZnO growth so as to avoid the step of seed layer coating. Besides, the zinc foil may serve as conductive substrate for certain practical applications of ZnO nanoarrays such as field emission and piezoelectric devices. Here, two kinds of masks derived from polystyrene (PS) MCC on zinc foils, which were denoted as inverted MCC (IMCC) and connected MCC (CMCC), were used for the patterned growth of ZnO, as illustrated in Figure 1. For the preparation of the IMCC mask, silica instead of photoresist was used to replicate the MCC film so as to avoid the cracks often caused by photoresist when subjected to hydrothermal conditions. ZnO will grow on the unmasked area of zinc foils (i.e., growth windows), resulting in nanopillar arrays. The size and spacing of the growth windows can be easily tuned by varying the size of the original colloidal spheres in the IMCC case or the interstice size between neighboring colloidal spheres in the CMCC case. The morphology of the ZnO at an individual growth site can be controlled by growth conditions such as reaction time and solution concentration. Moreover, this

(17) Hwang, W.; Choi, J.-H.; Kim, T. H.; Sung, J.; Myoung, J.-M.; Choi, D.-G.; Sohn, B.-H.; Lee, S. S.; Kim, D. H.; Park, C. *Chem. Mater.* **2008**, *20*, 6041.
(18) Rybczynski, J.; Banerjee, D.; Kosiorek, A.; Giersig, M.; Ren, Z. F. *Nano Lett.* **2004**, *4*, 2037.
(19) Wang, X.; Summers, C. J.; Wang, Z. L. *Nano Lett.* **2004**, *4*, 423.
(20) Liu, D. F.; Xiang, Y. J.; Wu, X. C.; Zhang, Z. X.; Liu, L. F.; Song, L.; Zhao, X. W.; Luo, S. D.; Ma, W. J.; Shen, J.; Zhou, W. Y.; Wang, G.; Wang, C. Y.; Xie, S. S. *Nano Lett.* **2006**, *6*, 2375.
(21) Liu, D. F.; Xiang, Y. J.; Zhang, J. P.; Wu, X. C.; Zhang, Z. X.; Liu, L. F.; Ma, W. J.; Shen, J.; Zhou, W. Y.; Xie, S. S. *Nanotechnology* **2007**, *18*, 405303.
(22) Vayssieres, L. *Adv. Mater.* **2003**, *15*, 464.
(23) Xu, S.; Wei, Y.; Kirkham, M.; Liu, J.; Mai, W.; Davidovic, D.; Snyder, R. L.; Wang, Z. L. *J. Am. Chem. Soc.* **2008**, *130*, 14958.
(24) Kim, Y.-J.; Lee, C.-H.; Hong, Y. J.; Yi, G.-C. *Appl. Phys. Lett.* **2006**, *89*, 163128.
(25) Cui, J.; Gibson, U. *Nanotechnology* **2007**, *18*, 155302.
(26) Weintraub, B.; Deng, Y.; Wang, Z. L. *J. Phys. Chem. C* **2007**, *111*, 10162.
(27) Ahsanulhaq, Q.; Kim, J. H.; Hahn, Y.-B. *Nanotechnology* **2007**, *18*, 485307.
(28) Matsuu, M.; Shimada, S.; Masuya, K.; Hirano, S.; Kuwabara, M. *Adv. Mater.* **2006**, *18*, 1617.
(29) Tak, Y.; Yong, K. *J. Phys. Chem. B* **2005**, *109*, 19263.
(30) Kwon, S. J.; Park, J.-H.; Park, J.-G. *Appl. Phys. Lett.* **2005**, *87*, 133112.
(31) Wang, C. H.; Wong, A. S. W.; Ho, G. W. *Langmuir* **2007**, *23*, 11960.
(32) Hsu, J. W. P.; Tian, Z. R.; Simmons, N. C.; Matzke, C. M.; Voigt, J. A.; Liu, J. *Nano Lett.* **2005**, *5*, 83.
(33) Morin, S. A.; Amos, F. F.; Jin, S. *J. Am. Chem. Soc.* **2007**, *129*, 13776.
(34) Kim, J. H.; Andeen, D.; Lange, F. F. *Adv. Mater.* **2006**, *18*, 2453.
(35) Cole, J. J.; Wang, X.; Knuesel, R. J.; Jacobs, H. O. *Nano Lett.* **2008**, *8*, 1477.
(36) (a) Hulteen, J. C.; van Duyne, R. P. *J. Vac. Sci. Technol., A* **1995**, *13*, 1553. (b) Haynes, C. L.; van Duyne, R. P. *J. Phys. Chem. B* **2001**, *105*, 5599. (c) Li, Y.; Cai, W.; Duan, G. *Chem. Mater.* **2008**, *20*, 615.
(37) Tang, Q.; Zhou, W. J.; Shen, J. M.; Zhang, W.; Kong, L. F.; Qian, Y. T. *Chem. Commun.* **2004**, 712.
(38) Li, Z.; Ding, Y.; Xiong, Y.; Yang, Q.; Xie, Y. *Chem. Eur. J.* **2004**, *10*, 5823.
(39) Zhang, Z.; Yu, H.; Shao, X.; Han, M. *Chem. Eur. J.* **2005**, *11*, 3149.
(40) Wu, X.; Bai, H.; Li, C.; Luand, G.; Shi, G. *Chem. Commun.* **2006**, 1655.
(41) Fang, Y.; Pang, Q.; Wen, X.; Wang, J.; Yang, S. *Small* **2006**, *2*, 612.
(42) Lu, C.; Qi, L.; Yang, J.; Tang, L.; Zhang, D.; Ma, J. *Chem. Commun.* **2006**, 3551.
(43) Zhao, F.; Li, X.; Zheng, J.-G.; Yang, X.; Zhao, F.; Wong, K. S.; Wang, J.; Lin, W.; Wu, M.; Su, Q. *Chem. Mater.* **2008**, *20*, 1197.

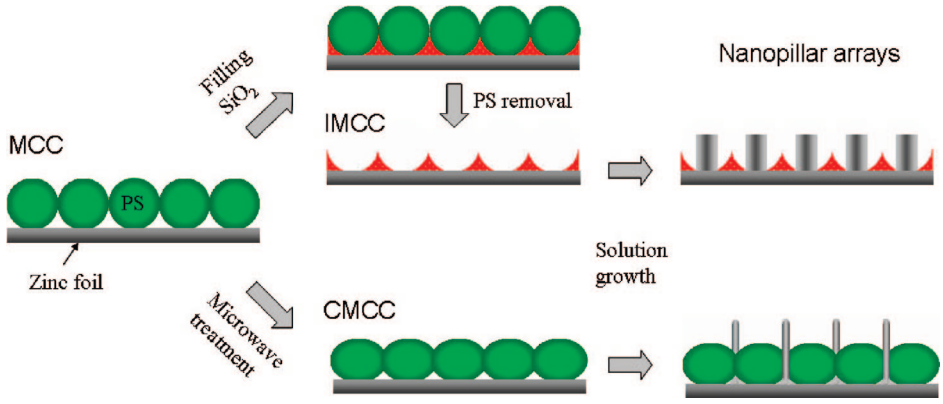

Figure 1. Schematic illustration of the fabrication process of ZnO nanopillar arrays in two different patterns.

method integrates the growth and assembly of well-separated ZnO nanocrystals in insulator cavities on conducting substrates simultaneously, providing a convenient way to fabricate nanodevices applicable in various areas such as stimulated emitters, actuators, and lasing cavities.

Experimental Section

Chemicals. Styrene (Beijing Chemical Co., 95%, washed in NaOH before use), potassium persulfate (Beijing Chemical Co., 99.5%), TEOS (tetraethoxysilane, Shantou Xilong Chemical Factory of China, Si·28%), zinc nitrate hexahydrate ($Zn(NO_3)_2 \cdot 6H_2O$, Sinopharm Chemical Reagent Co., Ltd., 99%), hexamethylene tetraammine (HMTA, $C_6H_{12}N_4$, Aldrich, 99%), and zinc foils (Alfa, 99.98%) were used.

Fabrication of IMCC and CMCC Patterns on Zinc Foils. Zinc foils were cut into squares of ~1 cm^2 and cleaned repeatedly in copious ethanol and acetone by sonication. The integration of monolayer colloidal crystal on a piece of square zinc foil was achieved using a method developed by Giersig et al.[44] with some modification. Specifically, a square glass of 1 cm^2, which was made hydrophilic by boiling in piranha solution (H_2SO_4:H_2O_2 = 7:3 v/v, *Caution!*), was placed at the mid-bottom of a Petri dish (Φ = 6 cm), and then ultrapure water was added carefully to the dish around the glass to level the edge of the upper surface of the glass but not cover the top of the glass. Monodisperse PS colloidal sphere (10 wt % aqueous dispersion) synthesized by emulsion-free polymerization[45] was diluted with an equal volume of ethanol. Then 12 μL of the dispersion was dropped on the top of the glass, which spread freely to cover nearly the whole water surface. Within a few seconds, a film with green color was formed on the water surface, indicating the formation of a monolayer of colloidal crystal. A few microliters of SDS solution (2 wt %.) was dropped onto the water surface to vary the surface tension. The film was packed closer and pushed to one side of the Petri dish and then quickly picked up by a piece of cleaned zinc foil. The zinc foil with monolayer colloidal crystals was kept in vacuum prior to use. To generate the inverted MCC (IMCC) mask on a zinc foil, the zinc foil with MCC was infiltrated with silica sol prepared according to a method reported previously.[46] After silification, IMCC on a zinc foil was obtained by extracting the PS MCC using toluene. To generate the connected MCC (CMCC) mask on zinc foils, the zinc foil with MCC was heat-treated in a mixed solvent (ethanol:acetone:water = 1: 1: 3, volume ratio) by pulsed microwave following a procedure described previously.[47] The extent of connection between neighboring spheres could be controlled by varying the number of pulse circles.

Wet Chemical Growth of ZnO on Patterned Zinc Foils. For the growth of ZnO nanostructures on the patterned zinc foils, $Zn(NO_3)_2$ and HMTA were used as reacting agents in aqueous solution.[48] Typically, equimolar aqueous solution of $Zn(NO_3)_2$ (0.1 M) and HMTA (0.1 M) were quickly mixed at room temperature, and then a piece of prepatterned zinc foil was put into the mixture with the pattern side up. The reaction vessel was sealed and kept at 80 °C for a certain time (typically 3 h). Then, the zinc foil was taken out, rinsed in ethanol by sonicaton to remove ZnO deposited from bulk solution, and finally dried in air for characterization. Ultrapure water produced from a Milli-Q academic system (−18.2 mΩ) was used in all experiments.

Characterization. Microstructures of the samples were studied by field-emission scanning electronic microscopy (SEM, Hitachi FE-S4800, 5kV), transmission electronic microscopy (TEM, JEOL JEM 200CX, 160 kV), selected area electron diffraction (SAED), and powder X-ray diffraction (XRD, Rigaku D/MAX-PC 2500, Cu Kα). A Renishaw InVia Raman fluorescence microscope was used for the measurement of Raman and the photoluminescence of ZnO nanoarrays at room temperature. The Raman spectroscope was first calibrated using a silicon plate. A 514.5 nm laser beam from argon ion was focused on a 2-μm spot on the ZnO sample plate. Photoluminescence measurement was carried out using a 324.5 nm He−Cd laser as the excitation source.

Results and Discussion

A silica IMCC film on a zinc foil was fabricated by replicating the prepared MCC of PS with silica, which was followed by extracting the PS spheres with toluene. The PS spheres in the MCC have an average diameter of 500 nm and arrange hexagonally on the zinc foil in a large area (Figure S1, Supporting Information). A typical SEM image of the as-replicated silica IMCC film is shown in Figure 2a, which shows a honeycomb-like structure, inheriting the long-range hexagonal order from the initial MCC template. A closer view shown in Figure 2b reveals that there is a circular area of bare zinc foil with a diameter of around 300 nm at the bottom of each cavity, which can serve as the active sites for the site-specific growth of ZnO nanopillars. Figure 2c shows a top view of the ZnO pillar arrays grown in an

(44) Rybczynski, J.; Ebels, U.; Giersig, M. *Colloids Surf., A* **2003**, *219*, 1.
(45) Holland, B. T.; Blanford, C. F.; Do, T.; Stein, A. *Chem. Mater.* **1999**, *11*, 795.
(46) Wang, L.; Yan, Q.; Zhao, X. S. *Langmuir* **2006**, *22*, 3481.
(47) Kosiorek, A.; Kandulski, W.; Glaczynska, H.; Giersig, M. *Small* **2005**, *1*, 439.
(48) Hirano, S.; Masuya, K.; Kuwabara, M. *J. Phys. Chem. B* **2004**, *108*, 4576.

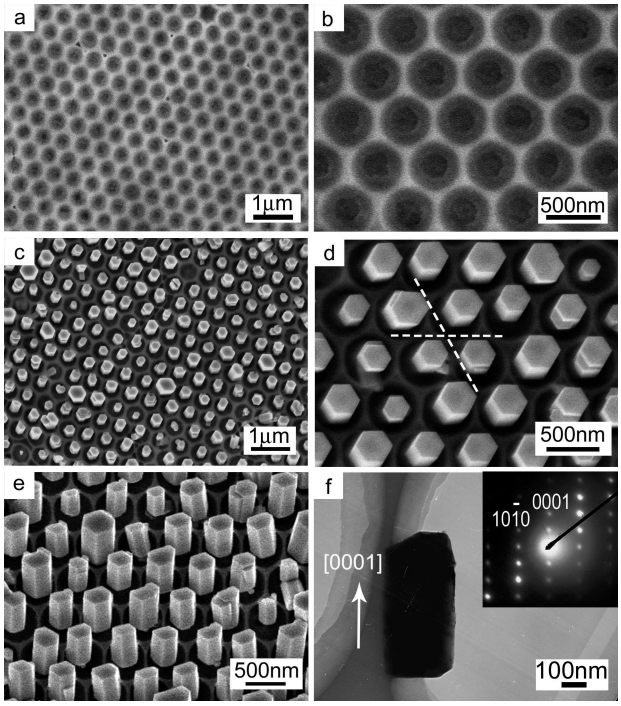

Figure 2. SEM images of silica IMCC templated by 500 nm PS spheres on zinc foil before (a, b) and after (c−e) the growth of ZnO nanopillar arrays and TEM image of a single ZnO nanopillar (f). Inset shows the related ED pattern.

aqueous solution containing 0.1 M $Zn(NO_3)_2$ and HMTA at 80 °C for 3 h. As can be seen, the orderly aligned pillars reserve the long-range hexagonal periodicity of the IMCC and the spacing between two neighboring pillars is 500 nm, as precisely predefined by the IMCC mask. From a magnified image shown in Figure 2d, we can see that the pillars are well-faceted hexagonal rods with a typical diameter of 300 nm and only one pillar is grown at one growth site. An oblique view shown in Figure 2e suggests that the vertically grown hexagonal pillars have a typical length of ∼600 nm, indicating an average aspect ratio of about 2 for each pillar. The well-faceted hexagonal morphology of the pillars indicates that each nanopillar is a single crystal of wurtzite ZnO with the elongation axis along the [0001] direction, which is further confirmed by the TEM image of a single nanopillar and the corresponding selected area electron diffraction (ED) pattern (Figure 2f).

Surprisingly, the hexagonally aligned hexagonal pillars are well oriented with their side faces parallel to each other, as denoted by the dashed lines in Figure 2d, indicating that the as-grown ZnO nanopillars are not only vertically well-aligned but are also side-oriented. It has been reported that side-oriented, hexagonally faceted single crystalline ZnO nanowire or nanopillar arrays can be obtained by epitaxial growth on prepatterned single-crystalline substrates that provide close lattice matching with ZnO by either hydrothermal growth[34,35] or metal-catalyzed vapor phase methods.[16,21] However, the phenomena of side-orientation among individual ZnO nanopillars has rarely been reported when ZnO seed layers or Zn foils were used as the substrates for the deposition of ZnO from solution. Moreover, side-orientation occurring in vapor phase growth is mostly caused by the interconnection at the roots of ZnO nanopillars, customarily due to the immigration

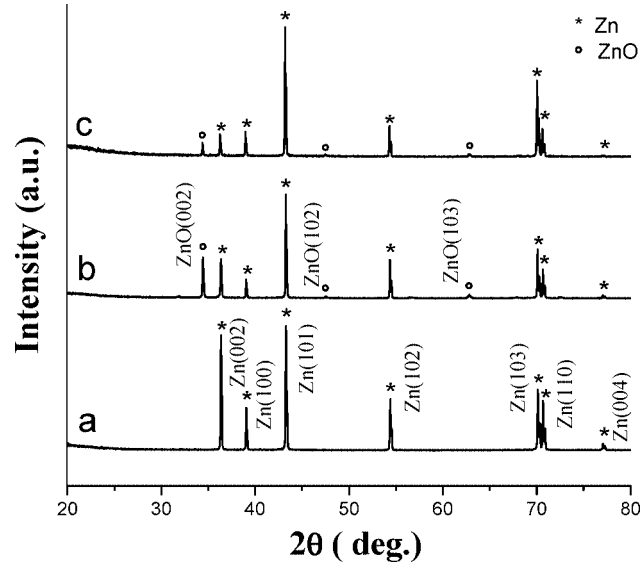

Figure 3. XRD patterns of bare zinc foil (a), ZnO dense layer grown on bare zinc foil (b), and ZnO nanopillar arrays grown on prepatterned zinc foil (c).

of the catalysts on substrates. So the as-grown pillars in those experiments are not genuinely well separated. TEM investigation of the scraped ZnO nanopillars from the zinc foil shows no visible interconnection between them in the present case (Figure S2, Supporting Information). To investigate the effect of the presence of the IMCC mask on the growth of ZnO, a control experiment in the absence of the mask using the same growth condition was performed. It was observed that a dense ZnO layer about 800 nm thick, which basically consisted of aggregated, well-crystallized hexagonal nanopillars with an average diameter of 500 nm, was grown on bare zinc foil (Figure S3, Supporting Information). Interestingly, the hexagonal nanopillars retain good vertical alignment and also show some side-orientation. This result indicates that the separated ZnO nanopillars could somehow communicate with each other to keep the identical crystal orientation, analogous to the case of epitaxial growth on specific single-crystalline substrates. A possible mechanism could be that the ultrathin oxide layer on the zinc foil played an important role in the side-oriented growth of ZnO crystals under such a solution reaction condition. In other words, although the silica walls surrounding the ZnO nanopillars kept the nanopillars well-separated, the ultrathin oxide layer on the zinc foil still connected, which may lead to the communication between ZnO nanopillars inside individual cavities, resulting in the side-oriented or quasi-epitaxial growth of ZnO nanopillars in a relatively large area. However, it remains largely unclear why the thin oxide layer on zinc foil may induce the quasi-epitaxial growth of ZnO nanopillars on the zinc foil. Much effort is required to investigate in detail the relationship between the structure of the oxide layer and the orientation of ZnO nanopillars to elucidate the exact mechanism.

The crystal structure and the orientation of the as-grown ZnO nanopillar arrays were revealed by the XRD investigation. Figure 3 shows the XRD patterns of the original bare zinc foil, the ZnO dense layer grown on the bare zinc foil, and the ZnO nanopillar arrays grown on the IMCC pre-

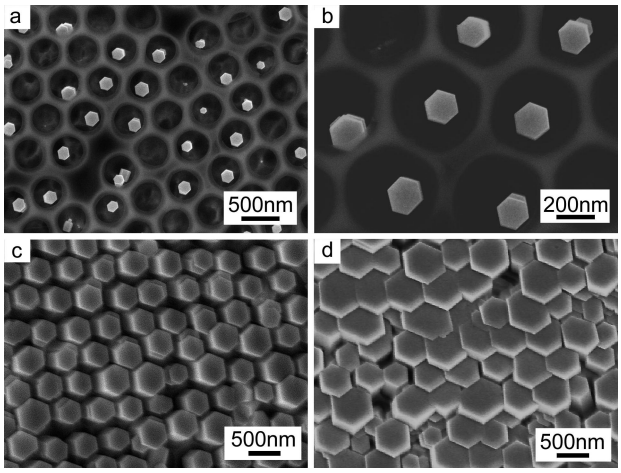

Figure 4. SEM images of ZnO nanopillar arrays obtained at varied reaction times at 80 °C: (a, b) 2 h, (c) 4 h, and (d) 6 h.

masked zinc foil. It can be seen that except for those ascribed to hexagonal Zn (JCPDS card No. 87-0713), the peaks can be indexed to the hexagonal wurtzite phase of ZnO (JCPDS card No. 89-1397). The as-grown ZnO nanopillar arrays show good crystallinity with a significantly intensified reflection of (002) at 36.4°, indicating a preferential orientation of the nanopillars with the *c* axis perpendicular to the zinc foil substrate. The diffraction peaks of the ZnO dense layers relative to the Zn diffraction peaks are stronger than those of the ZnO nanopillar arrays probably due to the larger quantity of deposited ZnO. The appearance of the weak (102) and (103) reflections of ZnO were probably caused by the uneven surface of the zinc foil.

To investigate the growth process of the ZnO nanopillars, the samples were taken out of the solution at different intervals of reaction time. Figure 4 shows the morphology evolution of ZnO nanopillar arrays with varied reaction times at 80 °C. Figure 4a shows that the well-separated ZnO nanopillars with diameters of 200 nm were obtained at 2 h, which grew individually at some growth sites. A magnified image shown in Figure 4b suggests that the hexagonal ZnO nanopillars are well-aligned with clear side-orientation. After 4 h, the pillars grew laterally, and the spacing of the pillar arrays became smaller than that of the product at 3 h (Figure 4c). When the reaction time was elongated to 6 h, the pillars overlapped with each other, resulting in the formation of a denser layer with well-recognizable hexagonal crystals, as shown in Figure 4d. In conclusion, by simply varying the reaction time, we can efficiently control the spacing between individual ZnO nanopillars, which has been considered important in certain applications such as field emission, where emitter spacing is very critical to the emission efficiency.[49] Unfortunately, the vertical growth in this case seems to be suppressed by the lateral growth, so the aspect ratio of the nanopillars cannot be increased by the elongation of reaction time.

It was found that a relatively high reaction solution concentration was essential for the individual growth mode, that is, one ZnO pillar at one growth site. While individually patterned ZnO nanopillar arrays were obtained at $[Zn(NO_3)_2]$ $=$ [HMTA] $=$ 0.1 M as shown in Figure 2, patterned arrays of ZnO nanorod bundles were obtained at relatively lower solution concentrations, which is shown in Figure 5. When the solution concentration was decreased to 0.02 M, a bundle of ZnO nanorods rather than one nanopillar grew from one single growth site, leading to a patterned array of vertically aligned ZnO nanorod bundles (Figure 5a,b). When the concentration was further decreased to 0.005 M, a patterned array of ZnO nanorod bundles was still obtained, but the overall diameter of a nanorod bundle inside one growth window became smaller and the diameter of each individual nanorod became smaller as well (Figure 5c,d). It has been reported that ZnO nanowires in close proximity are inclined to have coalescence effects, and multiple ZnO nanowires forming one single growth site may merge together to form a thicker nanowire under appropriate conditions.[23] The current result indicates that a relatively higher solution concentration may favor the individual growth mode rather than the multiple growth mode possibly due to the faster feeding of the reactant ions to the growth sites.

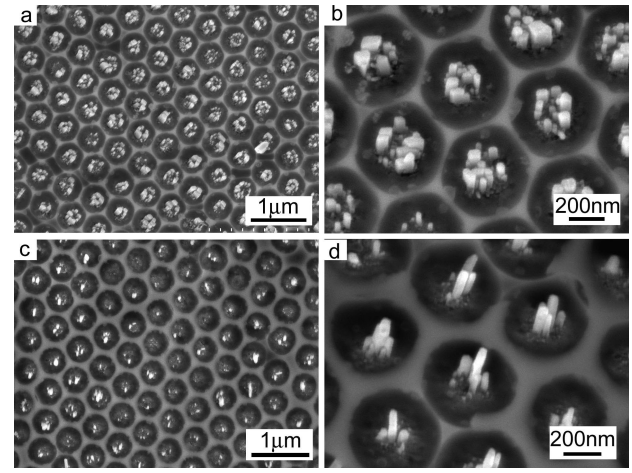

Figure 5. SEM images of ZnO nanorod bundles grown in lower solution concentrations at 80 °C for 3 h. $[Zn(NO_3)_2]$ $=$ [HMTA]: (a, b) 0.02 M and (c, d) 0.005 M.

The nanopillar width as well as the spacing of the individually patterned ZnO nanopillar arrays can be conveniently tuned by varying the PS sphere size of the original MCC template. For example, when the initial PS spheres of the MCC template was increased from 500 nm to 1 μm, silica IMCC with a cavity size of 1 μm were obtained (Figure 6a), and patterned arrays of individual ZnO pillars with a width of 910 nm were produced from the IMCC film under otherwise similar growth conditions (Figure 6b). Similarly, there was only one well-faceted hexagonal ZnO pillar grown from one growth window and the resultant pillar arrays were well-aligned with good side-orientation. These results demonstrated the flexibility of our approach to fabricate individually patterned ZnO nanopillar arrays with adjustable pillar width in the submicrometer range. And yet when a lower solution concentration (e.g., 0.05 M) was used, a bundle of ZnO nanorods grew in one cavity (Figure 6c), which indicates that the morphology at each growth site can be easily controlled by changing the concentration of the growth solution.

(49) Wang, X.; Zhou, J.; Lao, C.; Song, J.; Xu, N.; Wang, Z. L. *Adv. Mater.* **2007**, *19*, 1627.

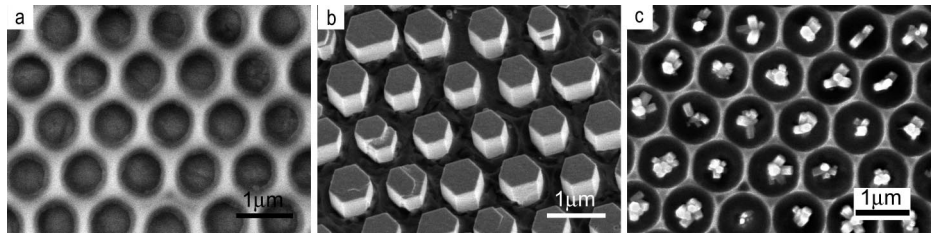

Figure 6. SEM images of silica IMCC templated by 1 μm PS spheres on zinc foil before (a) and after (b, c) the growth of ZnO nanoarrays. $[Zn(NO_3)_2] = [HMTA]$: (b) 0.1 M and (c) 0.05 M.

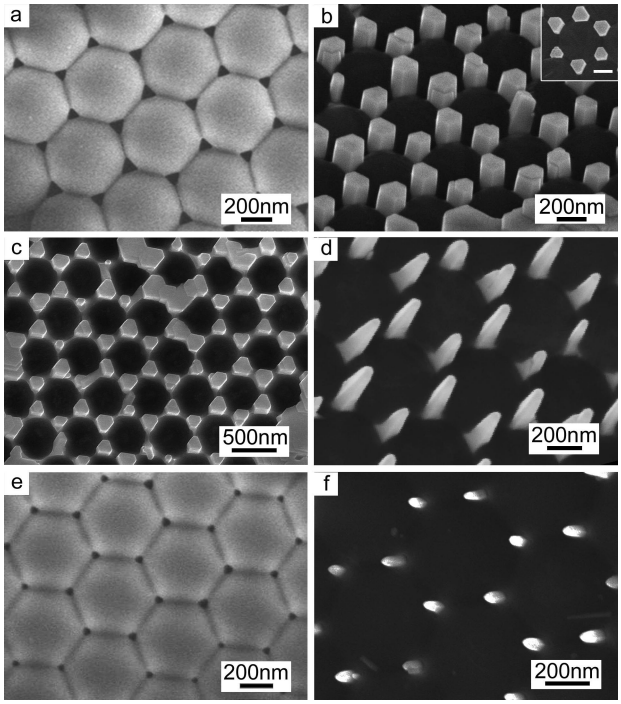

Figure 7. SEM images of PS CMCC template (a, e), ZnO nanopillar arrays grown from the CMCC mask with (b, d, f) and without (c) the PS spheres. $[Zn(NO_3)_2] = [HMTA]$: (b, c) 0.1 M, (d, f) 0.01 M. The scale bar in the inset is 200 nm.

Alternatively, individually patterned arrays of ZnO nanopillars can be prepared by using connected MCC (CMCC) of PS spheres as template (Figure 1). PS CMCC was obtained by annealing the PS MCC mask using pulsed microwave heating in a mixed solvent, which ensures the uniformity over the whole area of the sample and a good control over the aperture size. With increasing pulse numbers, the connection between neighboring spheres was aggravated, and thus the size of the apertures decreased. Figure 7a shows the PS CMCC on a zinc substrate after two pulse annealing. The aperture size of the CMCC mask, which is defined as the shortest distance between the point where two spheres touch and a point on the surface of the third sphere within a triangular aperture, was measured to be $\sim$ 95nm, considerably less than that of the original MCC template, that is, $\sim$140 nm (Figure S1, Supporting Information). After aging in reaction solution at 80 °C for 3 h, well-faceted hexagonal ZnO nanopillars with widths ranging from 120 to 180 nm grew perpendicularly from the uncovered apertures in an individual growth mode, that is, one ZnO pillar at one growth site (Figure 7b). Subsequent extraction of the polymer spheres resulted in the formation of patterned arrays of

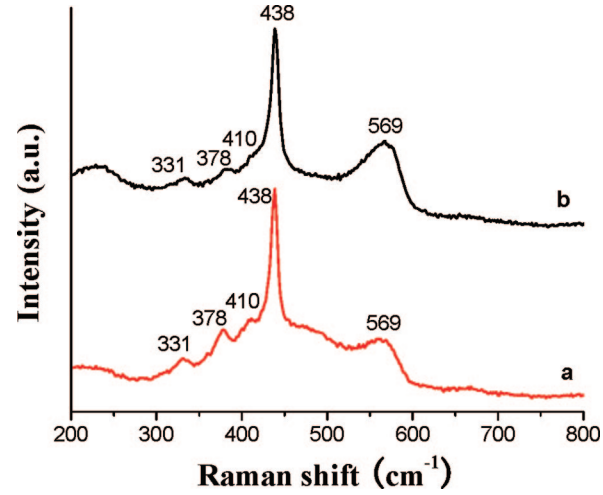

Figure 8. Room-temperature Raman spectra of ZnO nanopillar arrays (a) and dense layers (b) on zinc foil.

individual ZnO nanopillars on zinc foil (Figure 7c). However, it should be mentioned that it is very difficult to obtain perfect arrays of ZnO in a large area by this route because of the inherent structural defect of the mask, such as dislocations, vacancies, and cracks. Compared with the previous IMCC mask, the growth window size in the CMCC mask is generally smaller and can be easily decreased to the size range of tens of nanometers, which may be helpful for the growth of individually patterned arrays of ZnO nanopillars with smaller diameters. As expected, individual sharp pencil-like nanorods with a diameter about 110 nm grew from the triangular apertures at a lower reaction solution concentration (Figure 7d). Additionally, the diameter of the ZnO nanopillars can be tuned by varying the size of the aperture in the mask. For example, the aperture size was further decreased to 40 nm by an additional microwave pulse of the CMCC mask (Figure 7e) and then even thinner ZnO nanorods with a diameter of 60 nm could be obtained as a result (Figure 7f).

The good crystallinity of the as-synthesized ZnO nanopillar arrays was revealed by Raman scattering measurements that provided information on the vibrational properties of the samples. Raman spectra of the ZnO nanopillar arrays and the ZnO dense layers grown on zinc foil are presented in Figure 8, which shows that the two spectra are very similar. The remarkable E_{2H} mode of ZnO is located at 438 cm^{-1}, which corresponds to the characteristic band of the hexagonal wurtzite phase.[50] Weaker peaks at 331, 378, and 410 cm^{-1} can be assigned to the $3E_{2H}-E_{2\,L}$, $A_1(TO)$, and $E_1(TO)$ modes of ZnO, respectively. In addition, the peak located at 569 cm^{-1} can be attributed to the $E_1(LO)$ mode, which is associated with oxygen deficiency.[50] As can be seen, the 569

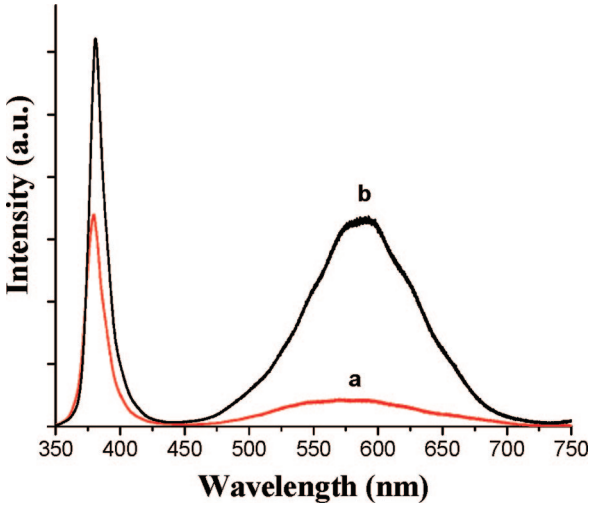

Figure 9. Room-temperature photoluminescence spectra of ZnO nanopillar arrays (a) and dense layers (b) on zinc foils.

cm^{-1} peak of the ZnO nanopillar arrays is less prominent than that of the ZnO dense layers, indicating a lower oxygen defect density.

The wide-range applications of UV emission in photonic devices have made ZnO an important material in optoelectronic industries. To evaluate the optical quality of the obtained ZnO nanopillars on zinc foil, their photoluminesence (PL) spectrum was measured at room temperature using a 325 nm He−Cd laser as the excitation source. As shown in Figure 9a, the sample exhibits a strong UV emission at 381 nm along with a weak and broad green emission around 580 nm. Generally, the UV emission is attributed to the band edge emission resulting from the exciton recombination, and the green emission results from the recombination of electrons in singlely ionized oxygen vacancies with photoexcited holes.[51] It is worth noting that the UV emission peak is very sharp and has a narrow full width at half-maximum (fwhm) value of 16 nm, which is comparable to that of the 1D ZnO arrays synthesized via the high-temperature vapor phase route.[52] For comparison, the photoluminescence of the ZnO dense layer on zinc foil was also measured, which is shown in Figure 9b. It can be seen that the ZnO dense layer has a relatively stronger UV emission due to a larger ZnO density on the substrate, but meanwhile it exhibits a prominent green emission, indicating considerably higher oxygen defects. It suggests that the ZnO nanopillar arrays have a higher optical quality relative to the ZnO dense layer, which can be attributed to a decrease in defect density due to the formation of spatially well-separated ZnO nanopillars. With strong excitonic emission as well as the well-defined structure, the ZnO nanopillars may find applications in stimulated emitters, actuators, and lasing cavities, where ZnO nanowires with diameters in the range of 150−500 nm are considered more suitable than sub-150-nm nanowires.[6b,16]

Conclusions

Individually patterned arrays of vertically aligned, side-oriented, hexagonal ZnO nanopillars have been successfully fabricated on zinc foils via a wet chemical route by templating of two patterned masks deriving from monolayer colloidal crystal (MCC), i.e., the inverted MCC and connected MCC. With the IMCC mask, the width and spacing of the ZnO nanopillar arrays can be efficiently tuned by varying the PS spheres size of the original MCC template or by elongating the reaction time. By this route, large-area patterned arrays of well-aligned ZnO nanopillars with diameters ranging from 200 to 900 nm, each of which grew individually from one single silica cavity on zinc substrate, can be readily produced. With the CMCC mask, the size and spacing of the ZnO nanopillars can also be adjusted by changing the aperture size of the CMCC mask and patterned arrays of nanopillars with thinner diameters (60−180 nm) can be obtained. Moreover, by decreasing the reaction solution concentration, a bundle of ZnO nanorods rather than an individual nanopillar were selectively grown at one single growth site. This work demonstrated a facile and efficient way for the production of individually patterned arrays of well-aligned ZnO nanopillars with a wide range of size and spacing. The as-integrated ZnO nanopillar arrays showed strong excitonic emission and weak defect-related emission at room temperature, which promises their potential applications in optical devices such as stimulated emitters and lasing cavities.

Acknowledgment. This work was supported by the NSFC (20873002, 20673007, 20633010, and 50821061), MOST (2007CB936201), and SRFDP (20070001018).

Supporting Information Available: SEM images of MCC of PS spheres, TEM image of ZnO nanopillars, and SEM images of the ZnO dense layer grown on bare zinc foil (PDF). This information is available free of charge via the Internet at http://pubs.acs.org.

CM802839U

(50) (a) Xing, Y. J.; Xi, Z. H.; Xue, Z. Q.; Zhang, X. D.; Song, J. H.; Wang, R. M.; Xu, J.; Song, Y.; Zhang, S. L.; Yu, D. P. *Appl. Phys. Lett.* **2003**, *83*, 1689. (b) Chen, S.; Liu, Y.; Shao, C.; Mu, R.; Lu, Y.; Zhang, J.; Shen, D.; Fan, X. *Adv. Mater.* **2005**, *17*, 586.
(51) Djurisic, A. B.; Leung, Y. H. *Small* **2006**, *2*, 944.
(52) Wen, X.; Fang, Y.; Pang, Q.; Yang, C.; Wang, J.; Ge, W.; Wong, K. S.; Yang, S. *J. Phys. Chem. B* **2005**, *109*, 15303.